

A note on the local discontinuous Galerkin method for linear problems in elasticity

Rommel Bustinza

ABSTRACT. In this paper we present a mixed local discontinuous Galerkin formulation for linear elasticity problems in the plane with Dirichlet boundary conditions. The approach follows previous dual-mixed methods and introduces the stress and strain tensors, and the rotation, as auxiliary unknowns. Next, we use suitable lifting operators to eliminate part of the unknowns of the corresponding discrete system, and obtain an equivalent variational formulation. We discuss about the unique solvability of the discrete scheme and the main difficulty that arises to derive the a-priori error estimates. Finally, we propose a computable a-posteriori error estimate and include some numerical examples, which show the expected rates of convergence for the error (with respect to a suitable mesh-dependent norm), as well as the good behaviour of the adaptivity algorithm to recover the optimal rates of convergence, results that are not covered yet by the theory.

1. Introduction

Discontinuous Galerkin (DG) method has been studied recently to solve different kind of problems coming from physics and engineering applications. We refer to [1] and references therein for an overview of the method. In addition, studies related to the use of DG methods for the Poisson, Stokes, Maxwell and Oseen equations can be found in [16], [7], [9], [10], and [11]. Concerning elasticity models, the nearly incompressible linear case has been studied in [14], [15] and [12], by applying different and known DG approaches, whose a-priori and/or a-posteriori results are still valid in the incompressible limit.

Among the advantages of using DG methods we can mention the fact that we can consider more general meshes (with hanging nodes, for e.g.) and different degrees of approximation per element, since inter-element continuity of the approximate solution is not strongly required. This latter property makes the DG methods suitable for the p

2000 *Mathematics Subject Classification*. Primary 65N30 Secondary 65N12.

Key words and phrases. Discontinuous Galerkin, a-priori and a-posteriori error estimates.

This research was partially supported by CONICYT-Chile through FONDECYT project No. 1050842 and by Dirección de Investigación of the Universidad de Concepción through the Advanced Research Groups Program.

and $h-p$ version, as well as for local adaptivity, subject that is still under development (see, e.g., [3], [5], [6], and [17]). On the other hand, the main disadvantage of this approach is the fact that the number of degrees of freedom is increased, which could be managed by performing some local adaptivity.

In this paper, we analyse the mixed local discontinuous Galerkin (LDG) method to solve (numerically) a linear incompressible elasticity model, with Dirichlet boundary conditions. In what follows, we present the model problem and give some discuss on it. First, we let Ω be a bounded and simply connected domain en \mathbb{R}^2 with polygonal boundary Γ . Then, the model problem consists in finding the displacement $\mathbf{u} := (u_1, u_2)^t$ and the pressure-like unknown p of an incompressible material occupying the region Ω , under the action of some external forces. Indeed, if $\boldsymbol{\sigma}(\mathbf{u}, p)$, $\mathbf{e}(\mathbf{u})$, and $\mathbf{I} \in \mathbb{R}^{2 \times 2}$ denote the Cauchy tensor, the strain tensor of small deformations, and the identity tensor, respectively, the constitutive equation is given by:

$$\boldsymbol{\sigma}(\mathbf{u}, p) = 2\mathbf{e}(\mathbf{u}) + p\mathbf{I} \quad \text{in } \Omega,$$

Then, given $\mathbf{f} \in [L^2(\Omega)]^2$ and $\mathbf{g} \in [H^{1/2}(\Gamma)]^2$, we look for $(\boldsymbol{\sigma}, \mathbf{u}, p)$ in appropriate spaces such that

$$(1.1) \quad \begin{aligned} \boldsymbol{\sigma} &= 2\mathbf{e}(\mathbf{u}) + p\mathbf{I} \quad \text{in } \Omega, & \mathbf{div} \boldsymbol{\sigma} &= -\mathbf{f} \quad \text{in } \Omega, \\ \mathbf{div} \mathbf{u} &= 0 \quad \text{in } \Omega, & \mathbf{u} &= \mathbf{g} \quad \text{on } \Gamma, \end{aligned}$$

where \mathbf{div} denotes the usual divergence operator \mathbf{div} acting along each row of the corresponding tensor. We point out that, due to the incompressibility of the material, the Dirichlet datum \mathbf{g} must satisfy the compatibility condition $\int_{\Gamma} \mathbf{g} \cdot \boldsymbol{\nu} = 0$, where $\boldsymbol{\nu}$ is the unit outward normal to Γ . From here on, given any Hilbert space S , we denote by S^2 and $S^{2 \times 2}$ the spaces of vectors and tensors of order 2, respectively, with entries in S , provided with the product norms induced by the norm of S . Also, for tensors $\mathbf{r} := (r_{ij})$, $\mathbf{s} := (s_{ij}) \in \mathbb{R}^{2 \times 2}$, and vectors $\mathbf{v} := (v_1, v_2)^t$, $\mathbf{w} := (w_1, w_2)^t \in \mathbb{R}^2$, we use the standard notation $\mathbf{r} : \mathbf{s} := \sum_{i,j=1}^2 r_{ij}s_{ij}$, and denote by $\mathbf{v} \otimes \mathbf{w}$ the tensor of order 2 whose ij th entry is $v_i w_j$. Note that the following identity holds: $\mathbf{v} \cdot (\mathbf{r}\mathbf{w}) = \mathbf{r} : (\mathbf{v} \otimes \mathbf{w})$.

We remark that a dual-mixed formulation of (1.1) based on enriched PEERS subspaces is proposed in [13], by introducing auxiliary unknowns such as $\mathbf{t} := \mathbf{e}(\mathbf{u})$ and ξ , which acts as a Lagrange multiplier, and using the identity $\mathbf{e}(\mathbf{u}) = \nabla \mathbf{u} - \boldsymbol{\gamma}$, with $\boldsymbol{\gamma} := \frac{1}{2}(\nabla \mathbf{u} - (\nabla \mathbf{u})^t) \in \mathcal{R} := \{\boldsymbol{\eta} \in [L^2(\Omega)]^{2 \times 2} : \boldsymbol{\eta} + \boldsymbol{\eta}^t = \mathbf{0}\}$. Then, following [13], our model (1.1) can be re-written as: Find $(\boldsymbol{\sigma}, \mathbf{t}, p, \mathbf{u}, \boldsymbol{\gamma})$ in appropriate spaces such that

$$(1.2) \quad \begin{aligned} \mathbf{t} &= \nabla \mathbf{u} - \boldsymbol{\gamma} \quad \text{in } \Omega, & \boldsymbol{\sigma} &= 2\mathbf{t} + p\mathbf{I} \quad \text{in } \Omega, & \mathbf{div} \boldsymbol{\sigma} &= -\mathbf{f} \quad \text{in } \Omega, \\ \text{tr}(\mathbf{u}) &= 0 \quad \text{in } \Omega, & \mathbf{u} &= \mathbf{g} \quad \text{on } \Gamma, \end{aligned}$$

We begin this work by extending and/or adapting the ideas developed in [6] to obtain a mixed LDG formulation for the model problem (1.2). Unfortunately we only can establish the uniqueness solvability of the discrete scheme, which motivates us to re-formulate the discrete variational formulation, considering suitable approximation

spaces for the (symmetric) tensors \mathbf{t} and $\boldsymbol{\sigma}$, and avoiding the introduction of the rotation $\boldsymbol{\gamma}$.

The rest of the paper is organized as follows. In Section 2 we derive a mixed local discontinuous Galerkin scheme, which includes the definition of the corresponding numerical fluxes and the reduced mixed formulation, discussing its solvability. Finally, an a-posteriori error estimate and some numerical experiments validating the good performance of the associated adaptive algorithm are reported in Section 3.

2. The LDG formulation

In this section, we derive a discrete formulation for the linear elasticity model (1.2), applying the local discontinuous Galerkin method and discuss about its solvability and well-posing.

2.1. Meshes. We let $\{\mathcal{T}_h\}_{h>0}$ be a family of shape-regular triangulations of $\bar{\Omega}$, each made up of straight-side triangles K with diameter h_K and unit outward normal to ∂K given by $\boldsymbol{\nu}_K$. As usual, the index h also denotes $h := \max_{K \in \mathcal{T}_h} h_K$. Then, given \mathcal{T}_h , its edges are defined as follows. An *interior edge* of \mathcal{T}_h is the (non-empty) interior of $\partial K \cap \partial K'$, where K and K' are two adjacent elements. A *boundary edge* of \mathcal{T}_h is the (non-empty) interior of $\partial K \cap \Gamma$, where K is a boundary element of \mathcal{T}_h . For each edge e , h_e represents its length. In addition, we define $E(K) :=$ edges of K , E_h^{int} : list of interior edges (counted only once) on Ω , E_h^Γ : list of edges on Γ , and I_h : interior grid generated by the triangulation, that is $I_h := \cup\{e : e \in E_h^{\text{int}}\}$. Also, we let Γ_h be the partition of Γ , inherited by \mathcal{T}_h . In addition, we also assume that \mathcal{T}_h is of *bounded variation*, which means that there exists $l > 1$, independent of the meshsize h , such that $l^{-1} \leq \frac{h_K}{h_{K'}} \leq l$ for each pair $K, K' \in \mathcal{T}_h$ sharing an interior edge.

2.2. Averages and jumps. Next, we define average and jump operators. To this end, let K and K' be two adjacent elements of \mathcal{T}_h and \mathbf{x} be an arbitrary point on the interior edge $e = \partial K \cap \partial K' \subset I_h$. In addition, let \mathbf{v} and $\boldsymbol{\tau}$ be vector-, and tensor-valued functions, respectively, that are smooth inside each element $K \in \mathcal{T}_h$. We denote by $(\mathbf{v}_{K,e}, \boldsymbol{\tau}_{K,e})$ the restriction of $(\mathbf{v}_K, \boldsymbol{\tau}_K)$ to e . Then, we define the averages at $\mathbf{x} \in e$ by:

$$\{\mathbf{v}\} := \frac{1}{2}(\mathbf{v}_{K,e} + \mathbf{v}_{K',e}), \quad \{\boldsymbol{\tau}\}_e := \frac{1}{2}(\boldsymbol{\tau}_{K,e} + \boldsymbol{\tau}_{K',e}).$$

Similarly, the jumps at $\mathbf{x} \in e$ are given by

$$\llbracket \mathbf{v} \rrbracket := \mathbf{v}_{K,e} \otimes \boldsymbol{\nu}_K + \mathbf{v}_{K',e} \otimes \boldsymbol{\nu}_{K'} \quad \llbracket \boldsymbol{\tau} \rrbracket_e := \boldsymbol{\tau}_{K,e} \boldsymbol{\nu}_K + \boldsymbol{\tau}_{K',e} \boldsymbol{\nu}_{K'}.$$

On boundary edges e , we set $\{\mathbf{v}\} := \mathbf{v}$, $\{\boldsymbol{\tau}\} := \boldsymbol{\tau}$, as well as , $\llbracket \mathbf{v} \rrbracket := \mathbf{v} \otimes \boldsymbol{\nu}$ and $\llbracket \boldsymbol{\tau} \rrbracket = \boldsymbol{\tau} \boldsymbol{\nu}$.

2.3. The global discrete formulation. Given a mesh \mathcal{T}_h , we proceed as in [6] and test each one of the unknowns (introduced at the introduction) by suitable test

functions. Then, we wish to approximate the solution of (1.1) by $(\mathbf{t}_h, \mathbf{u}_h, \boldsymbol{\sigma}_h, p_h, \boldsymbol{\gamma}_h, \xi_h) \in \boldsymbol{\Sigma}_h \times \boldsymbol{\mathcal{V}}_h \times \boldsymbol{\Sigma}_h \times \mathcal{W}_h \times \boldsymbol{\mathcal{R}}_h \times \mathbb{R}$, where

$$(2.1) \quad \begin{aligned} \boldsymbol{\Sigma}_h &:= \{ \mathbf{s} \in [L^2(\Omega)]^{2 \times 2} : \mathbf{s}|_K \in [\mathbf{P}_r(K)]^{2 \times 2} \quad \forall K \in \mathcal{T}_h \}, \\ \boldsymbol{\mathcal{V}}_h &:= \{ \mathbf{v} \in [H^1(\mathcal{T}_h)]^2 : \mathbf{v}|_K \in [\mathbf{P}_k(K)]^2 \quad \forall K \in \mathcal{T}_h \}, \\ \mathcal{W}_h &:= \{ q \in L^2(\Omega) : q|_K \in \mathbf{P}_{k-1}(K) \quad \forall K \in \mathcal{T}_h \}, \\ \boldsymbol{\mathcal{R}}_h &:= \{ \boldsymbol{\eta} \in \boldsymbol{\Sigma}_h : \boldsymbol{\eta}|_K + (\boldsymbol{\eta}|_K)^t = \mathbf{0} \quad \forall K \in \mathcal{T}_h \}, \end{aligned}$$

with integers $k \geq 1$ and $r \geq 0$. Hereafter, given an integer $m \geq 0$ we denote by $\mathbf{P}_m(K)$ the space of polynomials of total degree at most m on K . Also, the spaces $\boldsymbol{\Sigma}_h$, $\boldsymbol{\mathcal{R}}_h$ and \mathcal{W}_h are endowed with the respective and standard L^2 - norms, which for simplicity are denoted by $\|\cdot\|_{0,\Omega}$.

Then, defining the so-called numerical fluxes as in [6], we arise to the global discrete LDG formulation: Find $(\mathbf{t}_h, \mathbf{u}_h, \boldsymbol{\sigma}_h, p_h, \boldsymbol{\gamma}_h, \xi_h) \in \boldsymbol{\Sigma}_h \times \boldsymbol{\mathcal{V}}_h \times \boldsymbol{\Sigma}_h \times \mathcal{W}_h \times \boldsymbol{\mathcal{R}}_h \times \mathbb{R}$, such that

$$(2.2) \quad \begin{aligned} 2 \int_{\Omega} \mathbf{t}_h : \mathbf{s} - \int_{\Omega} \boldsymbol{\sigma}_h : \mathbf{s} + \int_{\Omega} p_h \operatorname{tr}(\mathbf{s}) &= 0, \\ \int_{\Omega} \mathbf{t}_h : \boldsymbol{\tau} - \left\{ \int_{\Omega} \nabla_h \mathbf{u}_h : \boldsymbol{\tau} - S(\mathbf{u}_h, \boldsymbol{\tau}) \right\} + \int_{\Omega} \boldsymbol{\gamma}_h : \boldsymbol{\tau} - \xi_h \int_{\Omega} \operatorname{tr}(\boldsymbol{\tau}) &= G(\boldsymbol{\tau}), \\ \left\{ \int_{\Omega} \boldsymbol{\sigma}_h : \nabla_h \mathbf{v} - S(\mathbf{v}, \boldsymbol{\sigma}_h) \right\} + \boldsymbol{\alpha}(\mathbf{u}_h, \mathbf{v}) &= F(\mathbf{v}), \\ \int_{\Omega} q \operatorname{tr}(\mathbf{t}_h) &= 0, \\ \int_{\Omega} \boldsymbol{\sigma}_h : \boldsymbol{\eta} &= 0, \\ \lambda \int_{\Omega} \operatorname{tr}(\boldsymbol{\sigma}_h) &= 0, \end{aligned}$$

for all $(\mathbf{s}, \mathbf{v}, \boldsymbol{\tau}, q, \boldsymbol{\eta}, \lambda) \in \boldsymbol{\Sigma}_h \times \boldsymbol{\mathcal{V}}_h \times \boldsymbol{\Sigma}_h \times \mathcal{W}_h \times \boldsymbol{\mathcal{R}}_h \times \mathbb{R}$. From here on, ∇_h denotes the piecewise gradient, and the bilinear forms $S : [H^1(\mathcal{T}_h)]^2 \times [L^2(\Omega)]^{2 \times 2} \rightarrow \mathbb{R}$ and $\boldsymbol{\alpha} : [H^1(\mathcal{T}_h)]^2 \times [H^1(\mathcal{T}_h)]^2 \rightarrow \mathbb{R}$, as well as the linear operators $G : [L^2(\Omega)]^{2 \times 2} \rightarrow \mathbb{R}$ and $F : [H^1(\mathcal{T}_h)]^2 \rightarrow \mathbb{R}$, are given by:

$$\begin{aligned} S(\mathbf{w}, \boldsymbol{\tau}) &:= \int_{\mathcal{E}_I} (\{\boldsymbol{\tau}\} - \llbracket \boldsymbol{\tau} \rrbracket \otimes \boldsymbol{\beta}) : \llbracket \mathbf{w} \rrbracket + \int_{\mathcal{E}_D} \mathbf{w} \cdot \boldsymbol{\tau} \boldsymbol{\nu}, \\ \boldsymbol{\alpha}(\mathbf{w}, \mathbf{v}) &:= \int_{\mathcal{E}_I} \boldsymbol{\alpha} \llbracket \mathbf{w} \rrbracket : \llbracket \mathbf{v} \rrbracket + \int_{\mathcal{E}_D} \boldsymbol{\alpha}(\mathbf{w} \otimes \boldsymbol{\nu}) : (\mathbf{v} \otimes \boldsymbol{\nu}), \\ G(\boldsymbol{\tau}) &:= \int_{\mathcal{E}_D} \mathbf{g} \cdot \boldsymbol{\tau} \boldsymbol{\nu}, \quad F(\mathbf{v}) := \int_{\Omega} \mathbf{f} \cdot \mathbf{v} + \int_{\mathcal{E}_D} \boldsymbol{\alpha}(\mathbf{g} \otimes \boldsymbol{\nu}) : (\mathbf{v} \otimes \boldsymbol{\nu}), \end{aligned}$$

for all $\mathbf{w}, \mathbf{v} \in [H^1(\mathcal{T}_h)]^2$ and $\boldsymbol{\tau} \in [L^2(\Omega)]^{2 \times 2}$.

The stabilization parameters α and β are chosen so that the solvability of the discrete LDG formulation is guaranteed. Therefore, we require that $\alpha \in P_0(I_h \cup \Gamma_h)$ and $\beta \in \mathbf{P}_0(I_h)$. Indeed, β can be chosen as the null vector. At this point, we introduce the energy-norm associated to \mathbf{V}_h

$$\|\mathbf{v}\|_h^2 := \|\nabla_h \mathbf{v}\|_{0,\Omega}^2 + |\mathbf{v}|_h^2 \quad \forall \mathbf{v} \in [H^1(\mathcal{T}_h)]^2,$$

where

$$|\mathbf{v}|_h^2 := \|\alpha^{1/2} \underline{[\mathbf{v}]}\|_{0,I_h}^2 + \|\alpha^{1/2} \mathbf{v} \otimes \boldsymbol{\nu}\|_{0,\mathcal{E}_D}^2 \quad \forall \mathbf{v} \in [H^1(\mathcal{T}_h)]^2,$$

2.4. A reduced mixed formulation. In what follows, we proceed as in [6] and obtain an equivalent reduced formulation to (2.2). In order to get this, we first notice that S and G are bounded. Indeed, there exists $C_S > 0$, independent of the meshsize, such that

$$|S(\mathbf{v}, \boldsymbol{\tau})| \leq C_S |\mathbf{v}|_h \|\boldsymbol{\tau}\|_{0,\Omega} \quad \forall (\mathbf{v}, \boldsymbol{\tau}) \in [H^1(\mathcal{T}_h)]^2 \times \boldsymbol{\Sigma}_h.$$

Therefore, we let $\mathbf{S}_h : [H^1(\mathcal{T}_h)]^2 \rightarrow \boldsymbol{\Sigma}_h$ be the linear and bounded operator induced by the bilinear form s , for which, given $\mathbf{v} \in [H^1(\mathcal{T}_h)]^2$, $\mathbf{S}_h(\mathbf{v})$ is the unique element in $\boldsymbol{\Sigma}_h$ (guaranteed by the Riesz representation Theorem) satisfying

$$\int_{\Omega} \mathbf{S}_h(\mathbf{v}) : \boldsymbol{\tau} = S(\mathbf{v}, \boldsymbol{\tau}) \quad \forall \boldsymbol{\tau} \in \boldsymbol{\Sigma}_h.$$

Analogously, we let \mathcal{G} be the unique element in $\boldsymbol{\Sigma}_h$ such that

$$\int_{\Omega} \mathcal{G} : \boldsymbol{\tau} = \int_{\mathcal{E}_D} \mathbf{g} \cdot \boldsymbol{\tau} \boldsymbol{\nu} \quad \forall \boldsymbol{\tau} \in \boldsymbol{\Sigma}_h.$$

We observe that if the displacement \mathbf{u} , that solves problem (1.1), belongs to $[H^t(\Omega)]^2$, with $t > 1$, then $\mathbf{S}_h(\mathbf{u}) = \mathcal{G}$. Moreover, applying a static condensation argument to the first two equations in (2.2), we deduce

$$\mathbf{t}_h = \Pi_{\boldsymbol{\Sigma}_h}(\nabla_h \mathbf{u}_h - \mathbf{S}_h(\mathbf{u}_h) + \mathcal{G} - \boldsymbol{\gamma}_h + \xi_h \mathbf{I}) \quad \text{and} \quad \boldsymbol{\sigma}_h = 2\mathbf{t}_h + p_h \mathbf{I},$$

where $\Pi_{\boldsymbol{\Sigma}_h}$ denotes the L^2 -projection operator onto $\boldsymbol{\Sigma}_h$. As in [6], we require that $\nabla_h \mathbf{v} \in \boldsymbol{\Sigma}_h$ for all $\mathbf{v} \in \mathbf{V}_h$, which is verified by considering $r = k$ or $r = k - 1$, and thus we obtain

$$(2.3) \quad \mathbf{t}_h = \nabla_h \mathbf{u}_h - \mathbf{S}_h(\mathbf{u}_h) + \mathcal{G} - \boldsymbol{\gamma}_h + \xi_h \mathbf{I} \quad \text{and} \quad \boldsymbol{\sigma}_h = 2\mathbf{t}_h + p_h \mathbf{I}.$$

After that, we introduce the bilinear forms $A_h : ([H^1(\mathcal{T}_h)]^2 \times \mathcal{R} \times \mathbb{R}) \times ([H^1(\mathcal{T}_h)]^2 \times \mathcal{R} \times \mathbb{R}) \rightarrow \mathbb{R}$ and $B_h : ([H^1(\mathcal{T}_h)]^2 \times \mathcal{R} \times \mathbb{R}) \times L^2(\Omega) \rightarrow \mathbb{R}$, which are defined, respectively, by

$$A_h((\mathbf{w}, \boldsymbol{\rho}, \mu), (\mathbf{v}, \boldsymbol{\eta}, \lambda)) := \boldsymbol{\alpha}(\mathbf{w}, \mathbf{v})$$

$$+ 2 \int_{\Omega} (\nabla_h \mathbf{w} - \mathbf{S}_h(\mathbf{w}) - \boldsymbol{\rho} + \mu \mathbf{I}) : (\nabla_h \mathbf{v} - \mathbf{S}_h(\mathbf{v}) - \boldsymbol{\eta} + \lambda \mathbf{I}),$$

and

$$B_h((\mathbf{v}, \boldsymbol{\eta}, \lambda), q) := \int_{\Omega} q \mathbf{I} : (\nabla_h \mathbf{v} - \mathbf{S}_h(\mathbf{v}) - \boldsymbol{\eta} + \lambda \mathbf{I}),$$

for all $\mathbf{w}, \mathbf{v} \in [H^1(\mathcal{T}_h)]^2$, $\boldsymbol{\rho}, \boldsymbol{\eta} \in \mathcal{R}_h$, $\mu, \lambda \in \mathbb{R}$, and $q \in \mathcal{W}$. In addition, we let $F_h : [H^1(\mathcal{T}_h)]^2 \times \mathcal{R} \times \mathbb{R} \rightarrow \mathbb{R}$ and $G_h : L^2(\Omega) \rightarrow \mathbb{R}$ be the linear functionals, defined by

$$F_h(\mathbf{v}, \boldsymbol{\eta}, \lambda) := F(\mathbf{v}) - \int_{\Omega} \boldsymbol{g} : (\nabla_h \mathbf{v} - \mathbf{S}_h(\mathbf{v}) - \boldsymbol{\eta} + \lambda \mathbf{I}) \quad \forall (\mathbf{v}, \boldsymbol{\eta}, \lambda) \in [H^1(\mathcal{T}_h)]^2 \times \mathcal{R} \times \mathbb{R},$$

and

$$G_h(q) := - \int_{\mathcal{E}_D} q \boldsymbol{g} \cdot \boldsymbol{\nu} \quad \forall q \in L^2(\Omega).$$

The next result establishes an equivalent formulation to (2.2).

LEMMA 2.1. *Let $(\mathbf{t}_h, \boldsymbol{\sigma}_h, p_h, \mathbf{u}_h, \boldsymbol{\gamma}_h, \xi_h) \in \boldsymbol{\Sigma}_h \times \boldsymbol{\Sigma}_h \times \mathcal{W}_h \times \mathcal{V}_h \times \mathcal{R}_h \times \mathbb{R}$ be a solution of (2.2). Then there holds*

(2.4)

$$\begin{aligned} A_h((\mathbf{u}_h, \boldsymbol{\gamma}_h, \xi_h), (\mathbf{v}, \boldsymbol{\eta}, \lambda)) + B_h((\mathbf{v}, \boldsymbol{\eta}, \lambda), p_h) &= F_h(\mathbf{v}, \boldsymbol{\eta}, \lambda) \quad \forall (\mathbf{v}, \boldsymbol{\eta}, \lambda) \in \mathcal{V}_h \times \mathcal{R}_h \times \mathbb{R}, \\ B_h((\mathbf{u}_h, \boldsymbol{\gamma}_h, \xi_h), q) &= G_h(q) \quad \forall q \in \mathcal{W}_h. \end{aligned}$$

Conversely, if $(\mathbf{u}_h, \boldsymbol{\gamma}_h, \xi_h, p_h) \in \mathcal{V}_h \times \mathcal{R}_h \times \mathbb{R} \times \mathcal{W}_h$ is a solution of (2.4), and \mathbf{t}_h and $\boldsymbol{\sigma}_h$ are defined by (2.3), then $(\mathbf{t}_h, \boldsymbol{\sigma}_h, \mathbf{u}_h, p_h, \boldsymbol{\gamma}_h, \xi_h)$ is a solution of (2.2).

Now, in order to prove the well-posedness of (2.4), we think of applying the Babuška-Brezzi theory. It is quite easy to check the inf-sup condition for B_h (its proof is very similar to that in Lemma 3.3 in [6]). Unfortunately, the coerciveness of A_h on $\text{Ker}(B_h)$ seems not to be verified, due to (up to the authors' knowledge) the inclusion of the rotation as an additional unknown. This motivates us to reformulate our problem (1.1), avoiding the introduction of the piecewise rotation $\boldsymbol{\gamma}_h$, considering the space

$$\boldsymbol{\Sigma}_h^s := \left\{ \mathbf{s} \in \boldsymbol{\Sigma}_h : \quad \mathbf{s}|_K = (\mathbf{s}|_K)^t \quad \forall K \in \mathcal{T}_h \right\}$$

to approximate the symmetric tensors $\boldsymbol{\sigma}$ and \mathbf{t} , instead of $\boldsymbol{\Sigma}_h$, and keeping the discrete spaces \mathcal{V}_h and \mathcal{W}_h as before. As a result, we derive another mixed LDG formulation, which is well-posed and has the optimal rates of convergence. The details of this work can be seen in [4], which applies this approach to solve a class of nonlinear problems in elasticity, containing as a by-product the linear case. Nevertheless, we still can prove the existence and uniqueness of the solution of (2.2), by checking that the solution of the corresponding homogeneous linear system is only the trivial one.

THEOREM 2.1. *Problem (2.2) has one and only one solution.*

PROOF. We consider the associated homogeneous linear system to (2.2). We know in advance that $\xi_h = 0$, $\mathbf{t}_h = \nabla_h \mathbf{u}_h - \mathbf{S}_h(\mathbf{u}_h) - \boldsymbol{\gamma}_h$, and $\boldsymbol{\sigma}_h = 2\mathbf{t}_h + p_h \mathbf{I}$. Next, testing the third, fourth and fifth equations in (2.2) by \mathbf{u}_h , $\boldsymbol{\gamma}_h$ and $p_h/2$, respectively, and after adding them and replacing $\boldsymbol{\sigma}_h$ in terms of \mathbf{u}_h , $\boldsymbol{\gamma}_h$ and p_h , we obtain that

$$2 \left\| \nabla_h \mathbf{u}_h - \mathbf{S}_h(\mathbf{u}_h) - \boldsymbol{\gamma}_h + \frac{p_h}{2} \mathbf{I} \right\|_{0,\Omega}^2 + |\mathbf{u}_h|_h^2 = 0,$$

which establishes that $\nabla_h \mathbf{u}_h - \mathbf{S}_h(\mathbf{u}_h) - \boldsymbol{\gamma}_h + \frac{p_h}{2} \mathbf{I} = \mathbf{0}$ and $\mathbf{u}_h \in C(\bar{\Omega})$ with $\mathbf{u}_h = \mathbf{0}$ on \mathcal{E}_D . Therefore, we have that $\mathbf{S}_h(\mathbf{u}_h) = \mathbf{0}$, $\boldsymbol{\gamma}_h = \frac{1}{2} (\nabla_h \mathbf{u}_h - (\nabla_h \mathbf{u}_h)^t)$, and

$e_{\mathcal{T}_h}(\mathbf{u}_h) + \frac{p_h}{2} \mathbf{I} = \mathbf{0}$, where $e_{\mathcal{T}_h}(\mathbf{v})$ denotes the piecewise symmetric part of $\nabla_h \mathbf{v}$, for each $\mathbf{v} \in [H^1(\mathcal{T}_h)]^2$. Then, we deduce that $\mathbf{t}_h = -\frac{p_h}{2} \mathbf{I}$, and since $\text{tr}(\mathbf{t}_h) = 0$ in each $K \in \mathcal{T}_h$, we conclude that $p_h = 0$, $\mathbf{t}_h = \mathbf{0} = \boldsymbol{\sigma}_h$, and $e_{\mathcal{T}_h}(\mathbf{u}_h) = \mathbf{0}$. Now, using the generalized Korn's inequality (cf. [2])

$$\|\nabla_h \mathbf{v}\|_{0,\Omega}^2 \leq C \left(\|e_{\mathcal{T}_h}(\mathbf{v})\|_{0,\Omega}^2 + |\mathbf{v}|_h^2 \right) \quad \forall \mathbf{v} \in [H^1(\mathcal{T}_h)]^2,$$

we find that $\nabla_h \mathbf{u}_h = \mathbf{0}$, which implies that $\mathbf{u}_h = \mathbf{0}$ and $\gamma_h = 0$. \square

3. Numerical Results

In this section we provide a numerical example illustrating the performance of the solvable LDG method (2.2). Hereafter, N denotes the number of degrees of freedom defining the subspace $\boldsymbol{\Sigma}_h \times \mathbf{V}_h \times \boldsymbol{\Sigma}_h \times \mathcal{W}_h \times \mathcal{R}_h \times \mathbb{R}$, that is $N := C_\kappa \times (\text{number of triangles of } \mathcal{T}_h) + 1$, with $C_\kappa = 16, 42$ for the $\mathbf{P}_0 - \mathbf{P}_1 - \mathbf{P}_0 - \mathbf{P}_0 - \mathbf{P}_0$ and $\mathbf{P}_1 - \mathbf{P}_2 - \mathbf{P}_1 - \mathbf{P}_1 - \mathbf{P}_1$ approximations, respectively. In addition, the global error is defined as follows

$$\mathbf{e} := \left\{ \|\mathbf{t} - \mathbf{t}_h\|_{0,\Omega}^2 + \|\mathbf{u} - \mathbf{u}_h\|_h^2 + \|\boldsymbol{\sigma} - \boldsymbol{\sigma}_h\|_{0,\Omega}^2 + |p - p_h|_{0,\Omega}^2 + \|\gamma - \gamma_h\|_{0,\Omega}^2 \right\}^{1/2},$$

where $(\mathbf{t}_h, \mathbf{u}_h, \boldsymbol{\sigma}_h, \gamma_h, p_h, \xi_h) \in \boldsymbol{\Sigma}_h \times \mathbf{V}_h \times \boldsymbol{\Sigma}_h \times \mathcal{W}_h \times \mathcal{R}_h \times \mathbb{R}$ is the unique solution of the discrete scheme (2.2). On the other hand, based on a previous work dealing with a class of nonlinear Stokes problems (cf. [6]), we propose the following a-posteriori error estimator

$$\vartheta := \left(\sum_{K \in \mathcal{T}_h} \vartheta_K^2 \right)^{1/2},$$

where for each $K \in \mathcal{T}_h$, ϑ_K is defined as

$$\begin{aligned} \vartheta_K^2 := & h_K^2 \|\mathbf{f} + \text{div}(2\mathbf{t}_h + p_h \mathbf{I})\|_{0,K}^2 + \|\alpha^{1/2} \llbracket \mathbf{u}_h \rrbracket\|_{0,\partial K \cap \mathcal{E}_I}^2 + \|\text{tr}(\mathbf{t}_h)\|_{0,K}^2 \\ & + h_K \|\llbracket 2\mathbf{t}_h + p_h \mathbf{I} \rrbracket\|_{0,\partial K \setminus \Gamma}^2 + h_K \|\boldsymbol{\sigma}_h - (2\mathbf{t}_h + p_h \mathbf{I})\|_{0,\partial K \cap \mathcal{E}_D}^2 + \|\boldsymbol{\sigma}_h - (2\mathbf{t}_h + p_h \mathbf{I})\|_{0,K}^2 \\ & + \|\alpha^{1/2} (\mathbf{u}_h - \mathbf{g}) \otimes \boldsymbol{\nu}\|_{0,\partial K \cap \mathcal{E}_D}^2 + h_K \|\{\boldsymbol{\sigma}_h\} - \llbracket \boldsymbol{\sigma}_h \rrbracket \otimes \boldsymbol{\beta} - \{2\mathbf{t}_h + p_h \mathbf{I}\}\|_{0,\partial K \cap \mathcal{E}_I}^2 + |K| |\bar{p}_h|^2, \end{aligned}$$

with \bar{p}_h being the mean value of p_h . The refinement strategy is described next ([19]):

- (1) Start with a coarse mesh \mathcal{T}_h .
- (2) Solve the discrete problem (2.2) for the current mesh \mathcal{T}_h .
- (3) Compute ϑ_K for each triangle $K \in \mathcal{T}_h$.
- (4) Evaluate stopping criterion and decide to finish or go to next step.
- (5) Apply *red-blue-green* procedure to refine each $K' \in \mathcal{T}_h$ whose error estimator $\vartheta_{K'}$ satisfies $\vartheta_{K'} \geq \frac{1}{2} \max\{\vartheta_K : K \in \mathcal{T}_h\}$.
- (6) Define resulting mesh as the current mesh \mathcal{T}_h and go to step 2.

Respect to the choices of the parameters α and $\boldsymbol{\beta}$, we point out that considering α independent of the meshsize (i.e of order $O(1)$), and proceeding as in [7] (see also [11]), we can obtain the same rates of convergence in energy norm for the displacement and the other unknowns than the obtained taking α of order $O(h^{-1})$. However, we are not able (at least theoretically) to recover the optimal rate of convergence for the L^2 -error

of the displacement, resulting in a loss of \sqrt{h} in its approximation. Furthermore, it has been shown in [8] that on Cartesian grids, with a special choice of the numerical fluxes (for which α is of order $O(1)$ and β is such that $|\beta \cdot \nu_K| = 1/2$) and for equal-order elements of bilinear polynomials, the LDG method super-converges. A similar phenomenon has not been observed on unstructured grids.

The numerical results presented below were obtained in a *Compaq Alpha ES40 Parallel Computer* using a MATLAB code, setting the parameters $\alpha = 1/h$ and $\beta = (1, 1)^t$ in the corresponding formulation, where the function $h \in L^\infty(I_h \cup \Gamma_h)$ is defined by $h(\mathbf{x}) = \min\{h_K, h_{K'}\}$, if $\mathbf{x} \in \text{int}(\partial K \cap \partial K')$, and by $h(\mathbf{x}) = h_K$ if $\mathbf{x} \in \text{int}(\partial K \cap \Gamma_h)$.

In addition, we test our results considering both regular meshes and meshes with *hanging nodes*, in which case our refinement algorithm is similar to the one described before, but instead of applying the *red-blue-green* procedure in step 5, we apply the *red* one.

We consider the L -shaped domain $\Omega := (-1, 1)^2 \setminus [0, 1]^2$, and choose \mathbf{f} and \mathbf{g} so that the exact solution is given by

$$\begin{cases} \mathbf{u}(\mathbf{x}) & := \left[(x_1 - 0.01)^2 + (x_2 - 0.01)^2 \right]^{-1/2} (x_2 - 0.01, 0.01 - x_1), \\ p(\mathbf{x}) & := \frac{1}{1.1 - x_1} - \frac{1}{3} \ln \left(\frac{441}{11} \right), \end{cases}$$

for all $\mathbf{x} := (x_1, x_2)^t \in \Omega$. We observe here that \mathbf{u} is divergence free in Ω and singular in an exterior neighborhood of $(0, 0)$. In addition, p is singular in an exterior neighborhood of the segment $\{1\} \times [0, 1]$. Figures 4.1 and 4.2 display the global errors \mathbf{e} , \mathbf{e}^{rgb} , and \mathbf{e}^r , corresponding to the uniform, red-blue-green, and red refinements, respectively, versus the degrees of freedom N (in a log-log scale). In all cases the errors of the adaptive methods decrease much faster than those of the uniform ones, recovering the order $O(h)$ and $O(h^2)$ for $\mathbf{P}_0 - \mathbf{P}_1 - \mathbf{P}_0 - \mathbf{P}_0 - \mathbf{P}_0$ and $\mathbf{P}_1 - \mathbf{P}_2 - \mathbf{P}_1 - \mathbf{P}_1 - \mathbf{P}_1$ approximations, respectively. Some intermediate adapted meshes, generated by different refinements, are displayed in Figures 4.3-4.6, showing that the adaptive algorithms are able to recognize the numerical singularities of \mathbf{u} and p . Moreover, we remark that the red refinement is more localized around the singularities than the blue-red-green one.

Finally, taking into account the numerical results, we can say that despite we are still not able to derive the a-priori error estimate, they show (at least numerically) that the rates of convergence of the errors are optimal, considering the regularity on the exact solution. Moreover, we point out that the proposed refinement algorithms are able to recover the optimal rate of convergence and/or improve the quality of the approximation, in presence of (numerical) singularities.

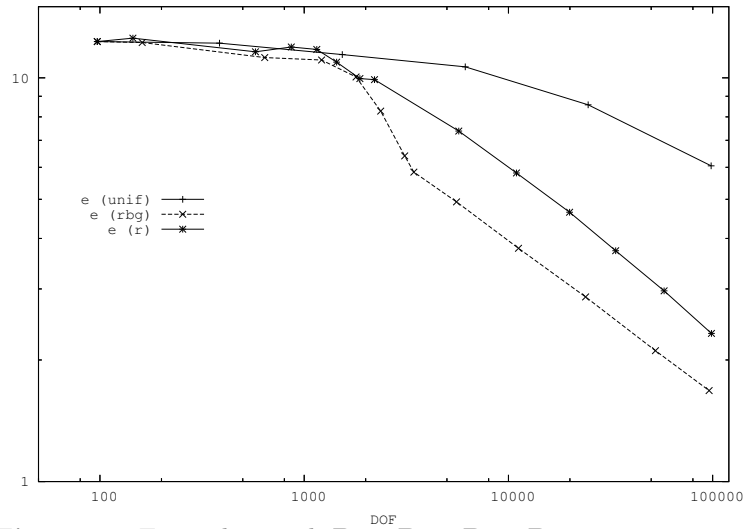


Figure 4.1 Example 1 with $\mathbf{P}_0 - \mathbf{P}_0 - \mathbf{P}_1 - \mathbf{P}_0$ approximation: global error \mathbf{e} for the uniform and adaptive refinements.

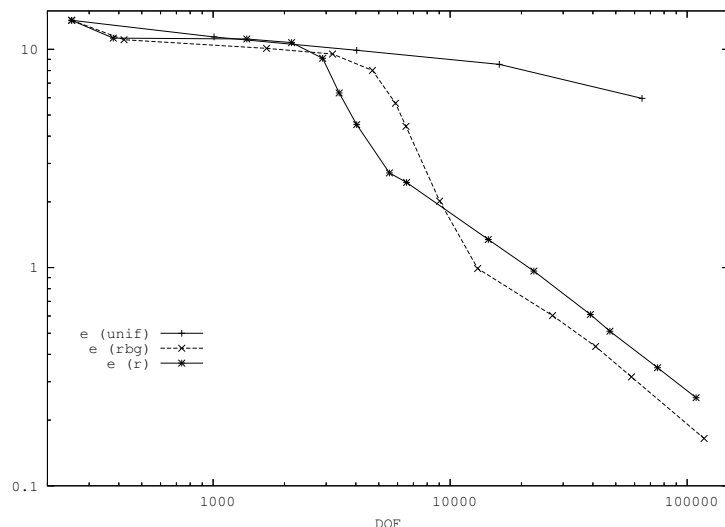


Figure 4.2 Example 1 with $\mathbf{P}_1 - \mathbf{P}_2 - \mathbf{P}_1 - \mathbf{P}_1 - \mathbf{P}_1$ approximation: global error \mathbf{e} for the uniform and adaptive refinements.

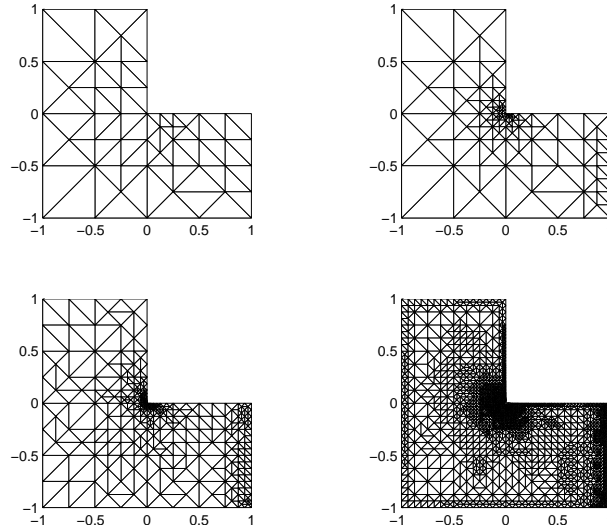


Figure 4.3 Example 1 with $\mathbf{P}_0 - \mathbf{P}_1 - \mathbf{P}_0 - \mathbf{P}_0 - \mathbf{P}_0$ approximation, without hanging nodes: adapted intermediate meshes with 1217, 3105, 11201 and 96017 degrees of freedom.

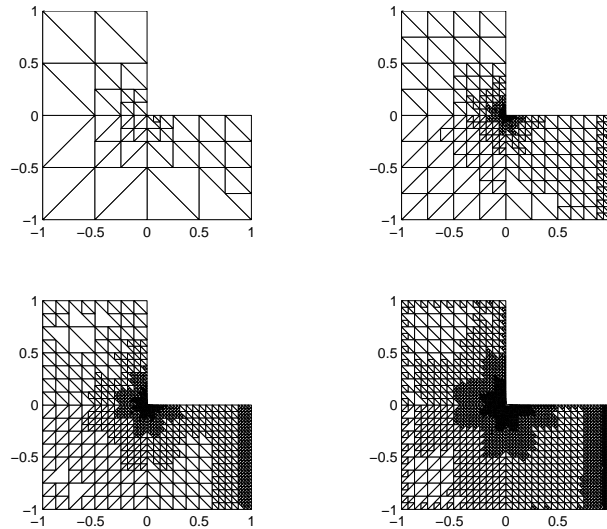


Figure 4.4 Example 1 with $\mathbf{P}_0 - \mathbf{P}_1 - \mathbf{P}_0 - \mathbf{P}_0 - \mathbf{P}_0$ approximation, with hanging nodes: adapted intermediate meshes with 1153, 10945, 33505 and 98689 degrees of freedom.

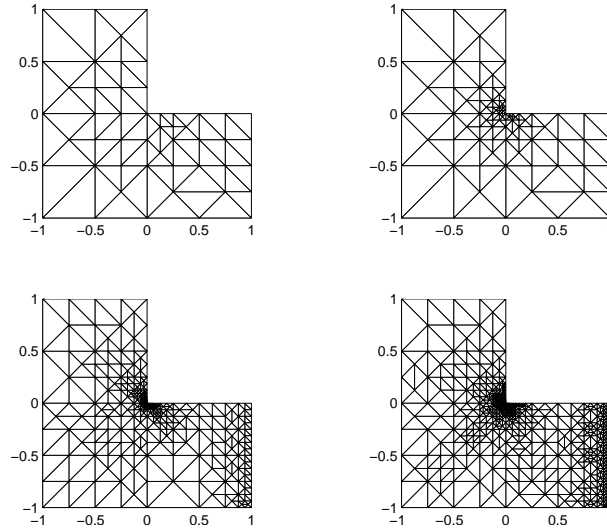


Figure 4.5 Example 1 with $\mathbf{P}_1 - \mathbf{P}_2 - \mathbf{P}_1 - \mathbf{P}_1 - \mathbf{P}_1$ approximation, without hanging nodes: adapted intermediate meshes with 3193, 6511, 27049 and 58255 degrees of freedom.

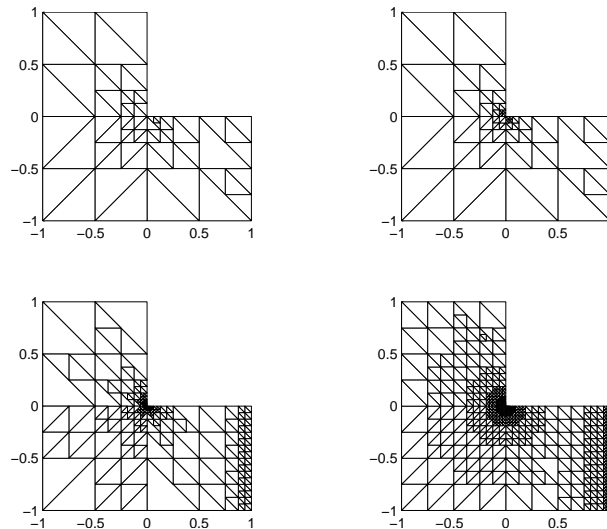


Figure 4.6 Example 1 with $\mathbf{P}_1 - \mathbf{P}_2 - \mathbf{P}_1 - \mathbf{P}_1 - \mathbf{P}_1$ approximation, with hanging nodes: adapted intermediate meshes with 2899, 4023, 14491 and 47251 degrees of freedom.

References

- [1] D.N. ARNOLD, F. BREZZI, B. COCKBURN, L.D. MARINI: *Unified analysis of discontinuous Galerkin methods for elliptic problems*. SIAM Journal on Numerical Analysis, vol. 39, 5, pp. 1749-1779, (2001).
- [2] D.N. ARNOLD, F. BREZZI AND L.D. MARINI: *A family of discontinuous Galerkin finite elements for the Reissner-Mindlin plate*. Journal of Scientific Computing, vol. 22, pp. 25-45, (2005).

- [3] R. BECKER, P. HANSBO AND M.G. LARSON: *Energy norm a posteriori error estimation for discontinuous Galerkin methods*. Computer Methods in Applied Mechanics and Engineering, vol. 192, pp. 723-733 (2003).
- [4] R. BUSTINZA: *Solving a class of nonlinear problems in elasticity using the local discontinuous Galerkin method*. Departamento de Ingeniería Matemática, Universidad de Concepción, (in preparation).
- [5] R. BUSTINZA, B. COCKBURN AND G.N. GATICA: *An a-posteriori error estimate for the local discontinuous Galerkin method applied to linear and nonlinear diffusion problems*. Journal of Scientific Computing, vol. 22, 1, pp. 147-185, (2005).
- [6] R. BUSTINZA AND G.N. GATICA: *A mixed local discontinuous Galerkin method for a class of nonlinear problems in fluid mechanics*. Journal of Computational Physics, vol. 207, pp. 427-456, (2005).
- [7] P. CASTILLO, B. COCKBURN, I. PERUGIA, AND D. SCHÖTZAU: *An a priori error analysis of the local discontinuous Galerkin method for elliptic problems*. SIAM Journal on Numerical Analysis, vol. 38, 5, pp. 1676-1706, (2000).
- [8] B. COCKBURN, G. KANSCHAT, I. PERUGIA, D. SCHÖTZAU: *Superconvergence of the local discontinuous Galerkin method for elliptic problems on Cartesian grids*. SIAM Journal on Numerical Analysis, vol. 39, pp. 264285, (2001).
- [9] B. COCKBURN, G. KANSCHAT AND D. SCHÖTZAU: *The local discontinuous Galerkin method for linear incompressible fluid flow: a review*. Computer and Fluids, vol. 34, pp. 491-506, (2005).
- [10] B. COCKBURN, G. KANSCHAT AND D. SCHÖTZAU: *The local discontinuous Galerkin method for the Oseen equations*. Mathematics of Computation, vol. 73, pp. 569-593, (2004).
- [11] B. COCKBURN, G. KANSCHAT, D. SCHÖTZAU AND C. SCHWAB: *Local discontinuous Galerkin methods for the Stokes system*. SIAM Journal on Numerical Analysis, vol. 40, 1, pp. 319-343, (2002).
- [12] B. COCKBURN, D. SCHÖTZAU AND J. WANG: *Discontinuous Galerkin methods for incompressible elastic materials*. Computer Methods in Applied Mechanics and Engineering, vol. 195, pp. 3184-3204, (2006).
- [13] G.N. GATICA AND E.P. STEPHAN: *A mixed-FEM formulation for nonlinear incompressible elasticity in the plane*. Numerical Methods for Partial Differential Equations, vol. 18, 1, pp. 105-128, (2002).
- [14] P. HANSBO AND M.G. LARSON: *Discontinuous Galerkin and Crouzeix-Raviart element: Application to elasticity*, Mathematical Modelling and Numerical Analysis, vol. 37, 1, pp. 63-72, (2003).
- [15] P. HOUSTON, D. SCHÖTZAU AND T.P. WIHLE: *An hp-adaptive mixed discontinuous Galerkin FEM for nearly incompressible linear elasticity*. Computer Methods in Applied Mechanics and Engineering, vol. 195, pp. 3224-3246, (2006).
- [16] I. PERUGIA AND D. SCHÖTZAU: *An hp-analysis of the local discontinuous Galerkin method for diffusion problems*. Journal of Scientific Computing, vol. 17, pp. 561-571, (2002).
- [17] B. RIVIERE AND M.F. WHEELER: *A posteriori error estimates and mesh adaptation strategy for discontinuous Galerkin methods applied to diffusion problems*. Computers & Mathematics with Applications, vol. 46, 1, pp. 141-163, (2003).
- [18] D. SCHÖTZAU, C. SCHWAB AND A. TOSELLI: *Mixed hp-DGFEM for incompressible flows*. SIAM Journal on Numerical Analysis, vol. 40, 6, pp. 2171-2194, (2003).
- [19] R. VERFÜRTH: *A Review of A Posteriori Error Estimation and Adaptive Mesh-Refinement Techniques*. Wiley-Teubner, Chichester, 1996.

Received 16 12 2005, revised 16 08 2006

^ADEPARTAMENTO DE INGENIERÍA MATEMÁTICA,
UNIVERSIDAD DE CONCEPCIÓN, CASILLA 160-C,
CONCEPCIÓN, CHILE.

E-mail address: `rbustinz@ing-mat.udec.cl`